

# Temporal Wheeler's delayed-Choice Experiment based on Cold Atomic Quantum Memory

Ming-Xin Dong,<sup>1,2</sup> Dong-Sheng Ding,<sup>1,2,\*</sup> Yi-Chen Yu,<sup>1,2</sup> Ying-Hao Ye,<sup>1,2</sup> Wei-Hang Zhang,<sup>1,2</sup>  
En-Ze Li,<sup>1,2</sup> Lei Zeng,<sup>1,2</sup> Kan Zhang,<sup>3</sup> Da-Chuang Li,<sup>4</sup> Guang-Can Guo,<sup>1,2</sup> and Bao-Sen Shi<sup>1,2,†</sup>

<sup>1</sup>Key Laboratory of Quantum Information, University of Science and Technology of China, Hefei, Anhui 230026, China.

<sup>2</sup>Synergetic Innovation Center of Quantum Information and Quantum Physics,  
University of Science and Technology of China, Hefei, Anhui 230026, China.

<sup>3</sup>Department of Fundamental Education, Anhui Institute of Information Technology, Wuhu, Anhui 241002, China.

<sup>4</sup>Institute for Quantum Control and Quantum Information and School of Physics and Materials Engineering,  
Hefei Normal University, Hefei, Anhui 230601, People's Republic of China.

(Dated: March 2, 2022)

Nowadays the most intriguing features of wave-particle complementarity of single photon is exemplified by the famous Wheeler's delayed choice experiment in linear optics, nuclear magnetic resonance and integrated photonic device systems. Studying the wave-particle behavior in light and matter interaction at single photon level is challenging and interesting, which gives how single photons complement in light and matter interaction. Here, we demonstrate a Wheeler's delayed choice experiment in an interface of light and atomic memory, in which the cold atomic memory makes the heralded single photon divided into a superposition of atomic collective excitation and leaked pulse, thus acting as memory beam-splitters. We observe the morphing behavior between particle and wave of a heralded single photon by changing the relative proportion of quantum random number generator, the second memory efficiency, and the relative storage time of two memories. The reported results exhibit the complementarity behavior of single photon under the interface of light-atom interaction.

The wave-particle duality or complementarity [1] in quantum physics has been demonstrated by Wheeler's delayed-choice experiment [2–8] exhibiting its paradoxical nature, in which a photon is forced to choose a behavior before the observer decides what to measure [9]. This wave-particle duality is the heart of quantum mechanics, because it is introduced to understand intuitively the behavior of quantum particles. Single photon's wave-particle duality are studied in many systems of linear optics [7, 10, 11] and integrated photonic device [12], in these experiments a Mach-Zender interferometer is configured in which a photon passing through it exhibits wave- or particle-like features depending on the experimental apparatus it is confronted by. By a proposal of using a 'quantum' beam splitter (BS) [13], people can investigate the intermediate behaviour between wave and particle nature [10–12]. Moreover, the delayed-choice quantum erasure [14, 15] and quantum entanglement swapping [16, 17] are reported with various

physical systems. Although the fundamental aspects of the delayed-choice experiments have been well studied in these systems, the delayed-choice experiment under the picture of light-matter interaction was rather obscure.

Light interaction with matter offers a rich of physics [18], such as photon absorption, spontaneous emission and photon storage and so on. One of interesting phenomena is quantum memory, a device that can coherently store and retrieve single photon including its information [19]. An intriguing question may arise as to what happens to wave-particle duality when light interact with matter. When a atom absorbs a single photon with less than one hundred percent, the question is whether the photon is leaked or absorbed by the atom is dependent on the choice of the observer.

In this work, we demonstrate a Wheeler's delayed-choice experiment based on atomic quantum memory. Here, three cold <sup>85</sup>Rb atomic ensembles trapped in a 2D magneto-optical trap are utilized, in which one ensemble is used to generate a heralded single photon and the other two act as the temporal beam splitters based on Raman storage protocol [20–23] configuring a temporal Mach-Zender interferometer. The memory we used here acts as a quantum device that divides the single photon packet into atomic and photonic components when the memory efficiency is less than unitary. We observe the morphing phenomenon between particle and wave behavior by changing a serial of experimental parameters. Our reported results give an important viewpoint that the single photon has a non-locality property under the interface of light and matter interaction.

The simple energy level diagram is shown in Fig. 1(a). We firstly generate a Stokes and anti-Stokes photon (Signal 2 and Signal 1) through spontaneously four-wave mixing (SFWM) [24, 25] process in MOT A, as shown in Fig. 1(b). Here, pump 1 (795 nm, Rabi frequency  $2\pi \times 1.19$  MHz) and pump 2 (780 nm, Rabi frequency  $2\pi \times 14.79$  MHz) are orthogonal polarization and propagate counter collinearly in MOT A with optical depth (OD) of 40. The angle between pump lasers and signals is  $2.8^\circ$ , and we collect the signal 2 (780 nm) and signal 1 (795 nm) by using lens with focal length of 300 mm.

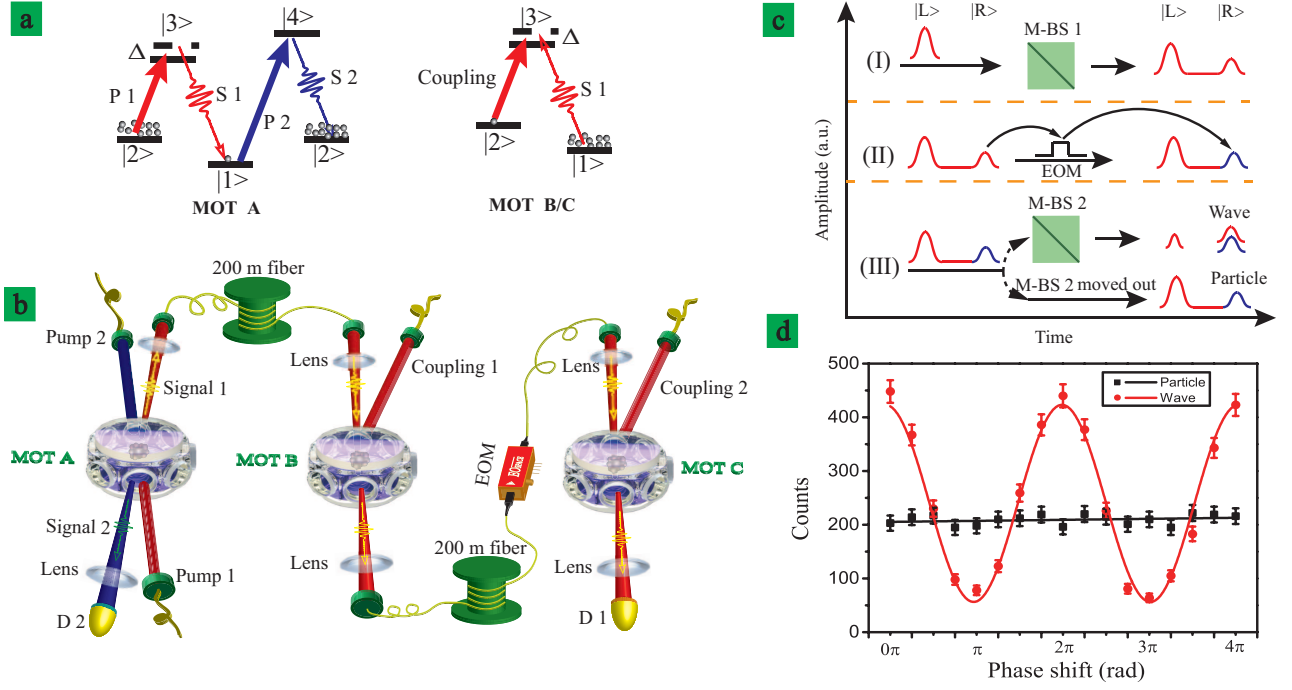


Figure 1. **Experimental realization of Wheeler's delayed-choice experiment.** (a) Energy level diagram. MOT A, B and C represent three magneto-optical traps. Single photons S 1 and S 2 are generated from MOT A using SFWM process, and the MOT B/C acting as quantum memory is based on Raman storage protocol with single-photon detuning  $\Delta/2\pi = 50$  MHz. States  $|1\rangle$ ,  $|2\rangle$ ,  $|3\rangle$  and  $|4\rangle$  correspond to  $^{85}\text{Rb}$  atomic levels of  $5S_{1/2}(F=2)$ ,  $5S_{1/2}(F=3)$ ,  $5P_{1/2}(F=3)$  and  $5P_{3/2}(F=3)$  respectively. (b) Simplified experimental setup. Pump 1/2 is pump light beam, Coupling 1/2 represents the coupling light beam. EOM is electro-optic modulator, introducing a phase shift, and 200 m fiber is used for optical delay of  $1\ \mu\text{s}$ . D 1/D 2, avalanche diode 1/2. (c) A simplified sketch of timing sequence in delayed-choice experiment. (d) The wave-particle duality of single-photon. When the M-BS 2 is inserted, the red experimental data dots are obtained and interference curve is fitted with a sine function, which is a wavelike phenomenon. The black line are fitted with a constant function while M-BS 2 is moved out, in which the interference is vanished, revealing a particle-like phenomenon.

Since signal 2 is detected the by single photon counting module (avalanche diode 2, PerkinElmer SPCM-AQR-15-FC, maximum dark count rate of 50/s), a heralded single photon signal 1 is obtained and then coupled into a 200-m single-mode fiber.

Quantum memory can be served as a quantum device that makes the photon pulse separate in timeline, the separated time interval and the amplitude can be arbitrarily configured, thus called as a dynamically configurable temporal BS [22]. Here we exploit two Raman memories MOT B and MOT C as memory-based beam splitters (M-BSs) to configure an interferometer in temporal domain. As depicted in Fig. 1(c), the implement of delayed-choice scheme is illustrated as follow. The Signal 1 photon is split into two parts by M-BS 1 with the following expressed state

$$|\psi\rangle = \sqrt{1 - \eta_{1con}} |L\rangle + e^{i\theta_1} \sqrt{\eta_{1con}} |R_{a1}\rangle \quad (1)$$

here,  $\eta_{1con}$ , is the conversion efficiency of optical signal to spin wave in MOT B. The right two terms in above equation represent the split states corresponding to the leaked part  $|L\rangle$  and stored part  $|R_{a1}\rangle$  under the quantum

memory process respectively, the coefficients  $\sqrt{1 - \eta_{1con}}$  and  $\sqrt{\eta_{1con}}$  are the amplitude of these two parts.  $\theta_1 = w \cdot \Delta t$  is the relative phase between the states  $|L\rangle$  and  $|R_{a1}\rangle$  with the storage time  $\Delta t$ . The stored part  $|R_{a1}\rangle$  corresponds to the atomic collective excited state defined in Methods. The expression given by Eq. (1) corresponds to superposition state of photon and atom, thus we don't know whether the photon is transformed to atomic state or is leaked.

After  $\Delta t = 200$  ns storage time, we turn on the coupling laser to read the spin wave in MOT B out as  $|R\rangle$ . Between MOT B and MOT C, we make signal travel through a 200-m fiber for optical delay of about  $1\ \mu\text{s}$  to enlarge the coherence length of interferometer (see Methods), the signal 1 photon has a photonic superposition  $|\psi_1\rangle \sim \sqrt{1 - \eta_{1con}} |L\rangle + \sqrt{\eta_1} e^{i\theta_1} |R\rangle$ . (Here,  $\eta_1 = \eta_{1con}\eta_{1stored}$ , is the total storage efficiency of optical signal in MOT B, including the efficiency of optical signal conversion to spin wave and spin wave retrieval to optical excitation  $\eta_{1stored}$ .) These two split photon packets distinct in time domain are equivalent to the two arms of interferometer. We vary the relative phase between two interferometer arms by modulating a phase shift on  $|R\rangle$

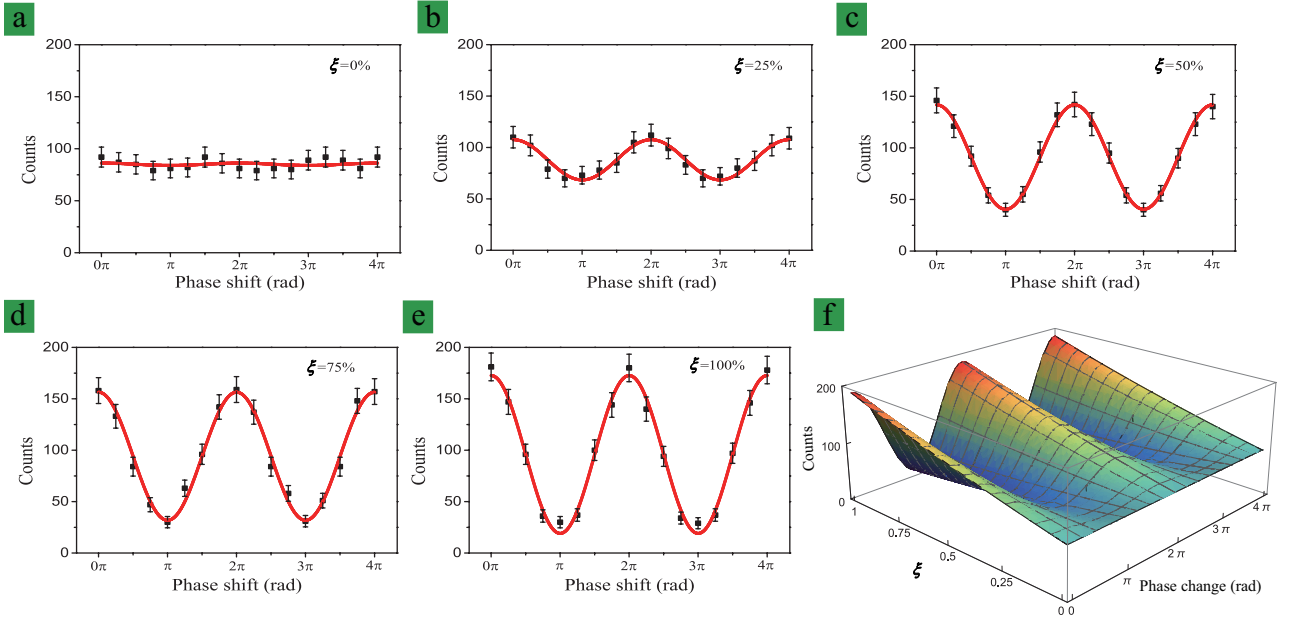


Figure 2. **Morphing phenomenon between particle and wave behavior.** (a)-(e) The recorded coincidence counts against varying the EOM phase in a step of  $\pi/4$ . The red curves are fitted  $N |\xi\sqrt{1-\eta_{1con}}\sqrt{\eta_2} + \sqrt{\eta_1}e^{i\varphi_{EOM}}|^2$ ,  $N$  is the total photon counts  $N = 611 \pm 32$ ,  $\eta_1 = 0.133 \pm 0.004$ ,  $\eta_{1con} = 0.850 \pm 0.026$ ,  $\eta_2 = 0.24$ . The fitted  $\xi$  is 0.01, 0.24, 0.53, 0.74, 0.96 from (a)-(e) respectively. (f) Simulated result of continuous morphing from wave to particle behavior with  $N = 611$ ,  $\eta_1 = 0.133$ ,  $\eta_{1con} = 0.850$ ,  $\eta_2 = 0.24$ .

by an electro-optical modulation (EOM), thus the state becomes

$$|\psi\rangle \sim \sqrt{1-\eta_{1con}}|L\rangle + \sqrt{\eta_1}e^{i\theta_1+\varphi_{EOM}}|R\rangle \quad (2)$$

here,  $\varphi_{EOM}$  is the added phase by EOM.

As soon as the leaked part arrives at M-BS 2 (in MOT C), a randomly choice to insert or remove the M-BS 2 has been made to realize the Wheeler's delayed choice experiment, which is controlled by a quantum random number generator (QRNG) with a density matrix  $\rho = (1-\xi)|0\rangle_{s2}\langle 0|_{s2} + \xi|1\rangle_{s2}\langle 1|_{s2}$ , the switch on or off for coupling 2 depends on states  $|0\rangle_{s2}$  and  $|1\rangle_{s2}$ . If M-BS 2 is removed/inserted ( $\xi = 0/1$ ), the whole setup forms an open/closed Mach-Zender interferometer, the leaked part is not-converted/converted to the spin wave in MOT C by switching off the coupling 2 light with Rabi frequency  $\Omega_{c2} = 2\pi \times 24.21$  MHz. The state is written as

$$|\psi\rangle \sim \sqrt{1-\eta_{1con}}\xi(\sqrt{1-\eta_{2con}}|L\rangle + \sqrt{\eta_{2con}}e^{i\theta_2}|R_{a2}\rangle) + \sqrt{1-\eta_{1con}}(1-\xi)|L\rangle + \sqrt{\eta_1}e^{i\theta_1+\varphi_{EOM}}|R\rangle \quad (3)$$

here,  $\eta_{2con}$  is the conversion efficiency of leaked part  $|L\rangle$  in Eq. (2) to spin wave in MOT C. After the same storage time of 200 ns, thus the relative phase  $\theta_1 = \theta_2 = \Delta\theta$ , we retrieve the spin wave to optical signal by considering the efficiency  $\eta_{2stored}$  of spin wave retrieval to optical excitation,

$$|\psi\rangle \sim (\sqrt{1-\eta_{1con}}\xi\sqrt{1-\eta_{2con}} + \sqrt{1-\eta_{1con}}(1-\xi))|L\rangle + e^{i\Delta\theta}(\xi\sqrt{1-\eta_{1con}}\sqrt{\eta_2}|R\rangle + \sqrt{\eta_1}e^{i\varphi_{EOM}}|R\rangle) \quad (4)$$

here,  $\eta_2 = \eta_{2con}\eta_{2stored}$  is the total storage efficiency of optical signal in MOT C, including the efficiency of optical signal conversion to spin wave and spin wave retrieval to optical excitation. We can check the photon interference by detecting the retrieved part  $|R\rangle$ , it osculates with a function of

$$P(\eta_1, \eta_2, \xi, \varphi_{EOM}) \sim |\xi\sqrt{1-\eta_{1con}}\sqrt{\eta_2} + \sqrt{\eta_1}e^{i\varphi_{EOM}}|^2 \quad (5)$$

In the first case, if M-BS 2 is inserted (for  $\xi = 1$ ), the two arms of interferometer are recombined and we can observe an wave-like phenomenon sketched in the red curve in Fig. 1(d). In the second case, while the M-BS2 is removed ( $\xi = 0$ ), the interferometer remains open, and we observe no interference, revealing the particle nature of photon, as shown in the black line in Fig. 1(d). In the second case, the open interferometer corresponds to the situation that the leaked part is not converted to spin wave and passes through the MOT C directly, in which we observe no interference because there is no overlap of split signals.

We demonstrate a morphing phenomenon between wave- and particle-like behavior by changing the rel-

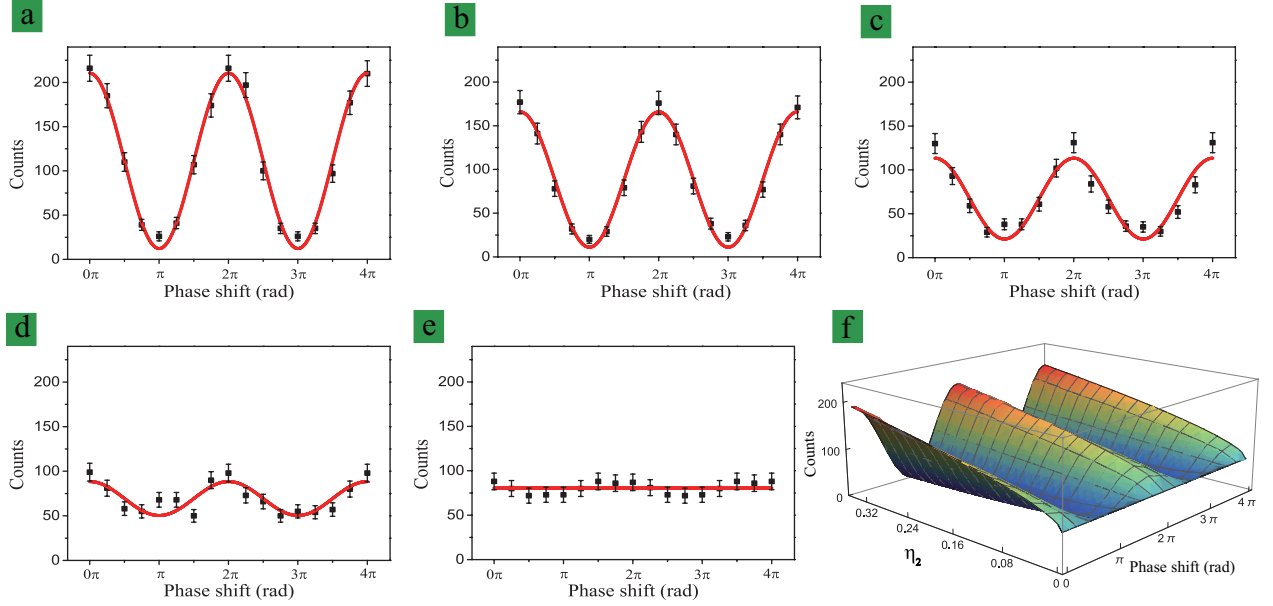


Figure 3. **Demonstration of interference ability of our interferometer.** (a)-(e) The interference pattern with different storage efficiency of spin wave in MOT C. The red curves are fitted  $N |\sqrt{1 - \eta_{1con}}\sqrt{\eta_2} + \sqrt{\eta_1}e^{i\varphi_{EOM}}|^2$  (where  $N = 568 \pm 40$ ,  $\eta_1 = 0.122 \pm 0.011$ ,  $\eta_{1con} = 0.850$ , from (a)-(e),  $\eta_2 = 0.331, 0.259, 0.114, 0.015, 0$  respectively). (f) The simulated interference ability of interferometer with the change of  $\eta_2$  (where we set  $N = 568$ ,  $\eta_1 = 0.122$ ,  $\eta_{1con} = 0.850$ ).

ative proportion of QRNG  $\xi = 0, 25, 50\%, 75\%, 1$ . Generally, a quantum delayed-choice experiments require an ancilla which is prepared in a superposition state  $|\Psi\rangle = \cos\alpha|0\rangle + \sin\alpha|1\rangle$  and then measured, the results controls the insert or remove of BS [10, 12], the morphing between wavelike and particle-like behavior is observed. In our scheme, the ancilla can be expressed as a mixed state  $\rho = (1 - \xi)|0\rangle\langle 0| + \xi|1\rangle\langle 1|$ , here  $(1 - \xi)$  is the probability of the vacuum state. In Fig. 2,  $\xi$  takes different values and we observe a phenomenon from particle to wave. The calculated visibility of interference is  $P(\eta_1, \eta_2, \xi, \varphi_{EOM})$ , and the measured visibility is not very high, this is caused by the mismatching of two retrieved signals because the bandwidth of two memories is slightly different from each other.

In an analog to operational definition given in [13], the “ability” or “inability” to generate interference can be utilized to describe the wave or particle properties. In the following part, we explore the relationship between interference ability of our apparatus and storage parameters such as storage efficiency and storage time, which is in favor of understanding wave-particle complementarity in the light-matter interaction. As illustrated in Fig. 3, the visibility is varied against different storage efficiencies in MOT C by varying the Rabi frequency of coupling 2 light from  $2\pi \times 27.86$  to 0. The maximum visibility (Fig. 3(a)) corresponds to the storage efficiency of 33.1% in MOT C. Here, in order to obtain the perfect interference, we should balance the retrieved signals after two storage processes. Therefore, we choose a suitable stor-

age efficiency of spin wave in MOT C by varying the Rabi frequency of coupling 2. In addition, it is also crucial to the choose a suitable storage efficiency in MOT B. Because if the storage efficiency in MOT B is too large, the leaked part as the input of the second storage process is too little to obtain the enough retrieved signal after leaving out of MOT C. As a result, in our experiment we actually optimize the storage efficiencies in MOT B and MOT C to achieve the best interference. The minimum visibility (Fig. 3(e)) corresponds to the MOT C storage efficiency of 0, revealing the nature of particle. Fig. 3(f) is the simulated interference against the effective storage efficiency of memory in MOT C.

In our scheme, it is intriguing to study the wave-particle complementarity using our controllable M-BS based on quantum memory. As a result, we attempt to vary the storage time of spin wave in MOT C and observe a morphing from wave to particle nature sketched in Fig. 4. The best interference pattern is shown in Fig. 4(c) with the storage time of 200 ns, which is identical to the storage time in MOT B. Intrinsically, the visibility of interference is positive correlated to the overlap among two retrieval signals. While we vary the storage time of spin wave in MOT C, the degree of two parts of signal 1 overlap in temporal domain is also changing. There is almost no interference pattern in Fig. 4(a/f) with the storage time of 160/280 ns, in which the two retrieved signals are almost separated with no overlap. The overlap time window is  $\sim 120$  ns ( $= 280 - 160$  ns), which is approach to the coherence time of retrieved optical mode

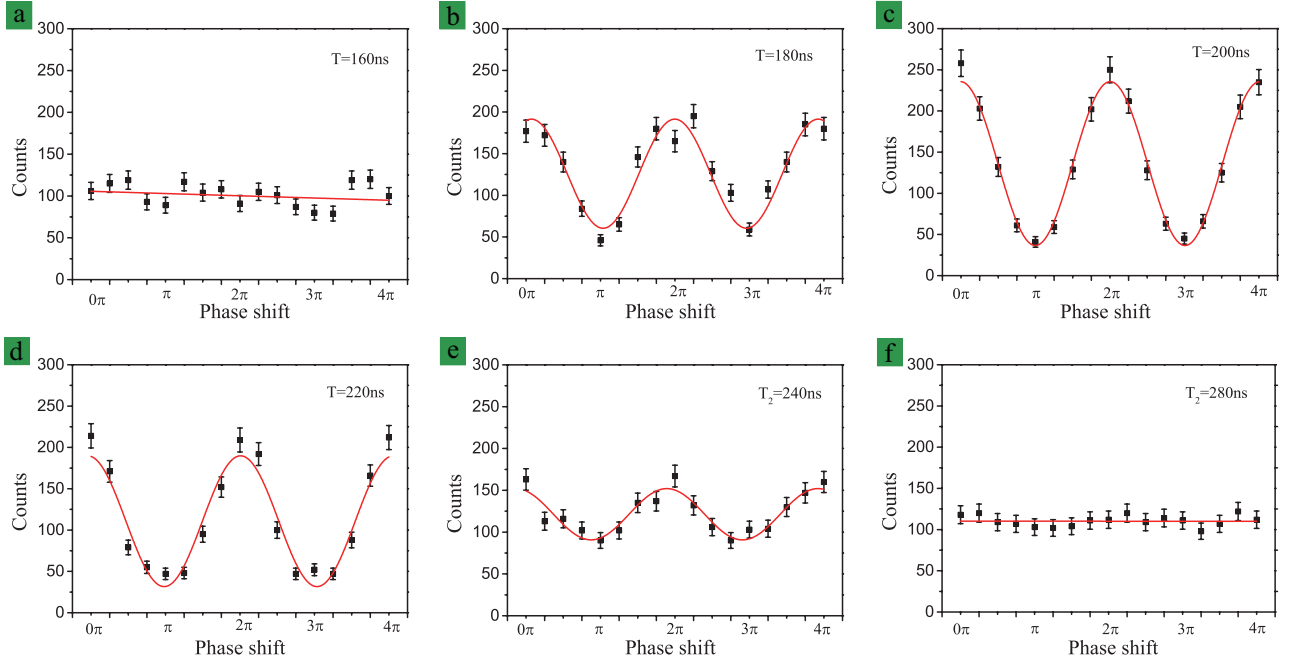


Figure 4. **The demonstration of quantum memory acting as the temporal BS.** (a)-(f) The interference phenomenon with different storage time of spin wave in MOT C from  $T=160$  ns to 280 ns. Dots are experimental data and red curves are fitted sine function or constant function.

of 110 ns. In addition, the overlap of two retrieved signals can also controlled by adjusting the waveforms or bandwidth of two retrieval wave packets.

In Fig. 5(a), the recorded coincidence counts with  $\Delta\Phi = 0$  and  $\Delta\Phi = \pi$  are illustrated in red and purple data respectively. The demonstration of wave and particle duality is not only dependent on the storage efficiencies  $\eta_1$  and  $\eta_2$ , but also the coherence of the M-BSs. To show the decoherence in our system, we explore the decoherence of two memories and interferometer respectively as shown in Fig. 5(b). The red and black curves describe the coherence of M-BS 1 in MOT B and M-BS 2 in MOT C with coherence time of 420 ns and 893 ns respectively. The blue curve is the coherence (with coherence time 691 ns) of interferometer when the phase of EOM  $\Delta\Phi = 0$ . Ultimately, we explore the relationship between OD of MOT C and interference visibility. Intrinsically, the change of OD of MOT C corresponds to the variation of storage efficiency in MOT C  $\eta_2$ . We vary the OD of MOT C from 0 to 40, meanwhile we measure the  $\eta_2$ . The visibility can be expressed as  $V = [P_{max} - P_{min}] / [P_{max} + P_{min}]$ , a function of  $\eta_2$ , and we fit it with our experimental data as shown in Fig. 5(c).

Our Wheeler's delayed-choice experiment rely on the key element of M-BS, its properties can be turned arbitrarily which are very different from other's demonstrations [10–12]. For example, the wave-particle duality demonstrated here is dependent on the pulse matching, the amplitude between two retrieved signals as described

in above. The bandwidth and amplitude of two retrieved signals can be turned by changing the OD in MOT B and MOT C and the Rabi frequencies  $\Omega_{c1}$  and  $\Omega_{c2}$ . In addition, the M-BS used here in principle can configure high-dimensional Mach-Zender interferometer with multiple temporal arms by addressing multipulse with a Raman quantum memory [22], by which, one can demonstrate the Wheeler's delayed-choice experiment with multiple photonic paths.

The QRNG used here is from the photon pair generated from SFWM process, which is a mixed state  $\rho = (1 - \xi) |0\rangle_{s2} \langle 0|_{s2} + \xi |1\rangle_{s2} \langle 1|_{s2}$ , not from a superposition state [10–12] or classical choices [3–8]. So the morphing phenomenon we measured correspond to the intermediate between quantum and classical situations. The intriguing physics here we want to emphasize is the complementarity of single photon interacted with quantum memory, exhibiting an important relationship between single photon and the atoms under interaction. The non-locality reported here is not only the two photonic temporal arms but also the states between atomic spin wave and the leaked signal.

In summary, we have demonstrated a Wheeler's delayed-choice experiment with Raman memory temporal beam splitters in two atomic ensembles, which construct a temporal Mach-Zender interferometer with a 200 meter fiber. The wave- and particle-like morphing behavior of heralded single photon is demonstrated by changing the experimental parameters of relative proportion, the storage efficiency, the optical depth and coherence of



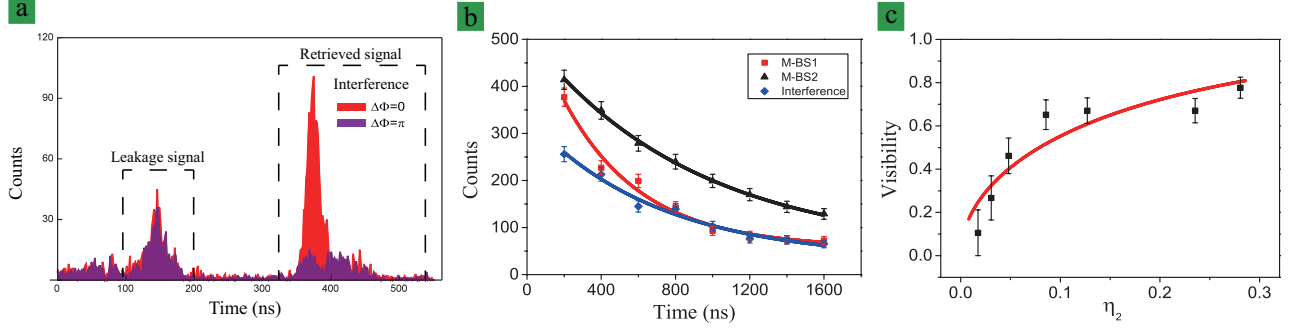


Figure 5. **The illustration of decoherence in our system.** (a) The interference of two spin waves stored in MOT B and MOT C with the modulated phase of 0 and  $\pi$  by EOM, corresponding to the red and blue parts respectively. (b) The recorded coincidence counts against storage time in MOT B (red), and MOT C (black). The red and black curves are fitted  $Ae^{-t/T_1} + g_0$  (where red curve,  $A = 503$ ,  $T_1 = 420$ ,  $g_0 = 58$ , and black curve,  $A = 457$ ,  $T_1 = 893$ ,  $g_0 = 51$ ). The interference results (blue) with modulated phase of EOM  $\Delta\Phi = 0$  against the storage time, here the storage time in MOT B and MOT C are set identically. The blue curve is also fitted  $Ae^{-t/T_2} + g_0$  (where  $A = 304$ ,  $T_2 = 691$ ,  $g_0 = 32$ ). (c) The interference visibility against the OD of atomic ensemble in MOT C. The red curve corresponds to theoretical fitting (where  $\eta_1 = 0.132$ ,  $\eta_{1con} = 0.88$ ).

the M-BSs. The resulting Wheeler’s delayed-choice experiment under light-atom interaction gives a fundamental aspect that the single photon exhibits a non-locality when interacting with atoms.

## METHOD SECTIONS

**Experimental time sequence.** The repetition rate of our experiment is 100 Hz, and the MOT trapping time is 8.7 ms. Moreover, the experimental window is 1.3 ms. The fields of pumps 1 and 2 are controlled by two acousto-optic modulators (AOMs) modulated by arbitrary function generator (Tektronix, AFG3252). Two lenses L1 and L2, each with a focal length of 300 mm, are used to couple the signal fields into the atomic ensemble in MOT 1. The fields of pumps 1 and 2 are collinear, and hence their respective signal fields are collinear, and hence their respective signal fields are collinear. The vector matching condition  $k_{p1} - k_{s1} = k_{p2} - k_{s2}$  is satisfied in the spontaneous four-wave mixing process, as the methods are the same as in our previous work. The two signal photons are collected into their respective single-mode fibers and are detected by two single photon detectors (avalanche diode, PerkinElmer SPCM-AQR-16-FC, 60 efficiency, maximum dark count rate of 25/s). The two detectors are gated in the experimental window. The gated signals from the two detectors are then sent to a time-correlated single photon counting system (TimeHarp 260) to measure their time-correlated function.

**Raman quantum memory.** Two atomic ensembles in MOT B and MOT C are serving as Raman memories [23]. The specific storage process is illustrated as follow: The signal 1 photon is directed through the MOT B with OD of 35, and simultaneously we adiabatically switch off the coupling 1 light with Rabi fre-

quency  $\Omega_{c1} = 2\pi \times 20.61$  MHz and a beam waist of 2 mm, and then a stored atomic collective excitation is obtained given by  $1/\sqrt{m} \sum e^{ik_S \cdot r_i} |1\rangle_1 \cdots |2\rangle_i \cdots |1\rangle_m$  [26], also called as spin wave.  $k_S = k_{c1} - k_{s1}$  is the wave vector of atomic spin wave,  $k_{c1}$  and  $k_{s1}$  are the vectors of coupling and signal 1 fields,  $r_i$  denotes the position of the  $i$ -th atom in atomic ensemble in MOT B. After a programmable storage time, the spin wave is converted back into photonic excitation by switching on the coupling 1 light again. Due to the Raman memory efficiency is significantly dependent on the OD of atoms [27], the input single photon would induces a leaked component in the storage process with a controllable OD.

**The coherence of Mach-Zender interferometer.** The two signal parts  $|L\rangle$ ,  $|R\rangle$  (leaked and retrieved signals) marked in Fig.1 (c) are exploited to construct the two arms of the temporal Mach-Zender interferometer. We enlarge the length of interferometer arms by inserting a 200-m optical fiber (corresponding to a time delay of  $\sim 1$   $\mu$ s) in signal 1’s optical path to avoid the retrieved signal interferes with itself on M-BS 2 if the length of interferometer arm is shorter than the coherence length of  $|R\rangle$ . The coherence length of  $|R\rangle$  is determined by the time width of the signal 1 photon, which is 50 ns for our experiment.

**Quantum random number generator.** We generate the random number by performing a logic gate operation between the detection of Stokes photon and a 100 kHz transistor-transistor logic (TTL) signal generated by an arbitrary function generator. Intrinsically, the emission of single photon is a SFWM process, the generated QRNG is described by the operator  $\rho = (1-\xi) |0\rangle_{s2} \langle 0|_{s2} + \xi |1\rangle_{s2} \langle 1|_{s2}$ , the coefficient  $\xi$  can be adjusted by the duty cycle of TTL signal, the first term  $(1-\xi) |0\rangle_{s2} \langle 0|_{s2}$  is used to switch the coupling 2 laser off

and the second term  $\xi |1\rangle_{s2} \langle 1|_{s2}$  to switch the coupling 2 laser on. We measure a morphing phenomenon of photon that behaves from wave to particle by changing the duty cycle of TTL signal.

**Author contributions** Ming-Xin Dong and Dong-Sheng Ding contribute to this paper equally. D.S.D. conceived the idea and experiment. M.X.D. designed and carried out the experiments with assistance from W.H.Z. and Y.C.Y.. M.X.D. wrote the manuscript with contributions from B.S.S.. D.S.D., B.S.S. and G.C.G. supervised the project.

**Competing financial interests** The authors declare no competing financial interests.

**Acknowledgments** This work was supported by National Key R&D Program of China (2017YFA0304800), the National Natural Science Foundation of China (Grant Nos. 61525504, 61722510, 61435011, 11174271, 61275115, 11604322), and the Innovation Fund from CAS, Anhui Initiative in Quantum Information Technologies (AHY020200).

---

\* dds@ustc.edu.cn

† drshi@ustc.edu.cn

- [1] W. Greiner, *Quantum mechanics: an introduction* (Springer Science & Business Media, 2011).
- [2] J. A. Wheeler, in *Mathematical foundations of quantum theory* (Elsevier, 1978) pp. 9–48.
- [3] T. Hellmuth, H. Walther, A. Zajonc, and W. Schleich, *Physical Review A* **35**, 2532 (1987).
- [4] J. Balduhn, E. Mohler, and W. Martienssen, *Zeitschrift für Physik B Condensed Matter* **77**, 347 (1989).
- [5] B. Lawson-Daku, R. Asimov, O. Gorceix, C. Miniatura, J. Robert, and J. Baudon, *Physical review A* **54**, 5042 (1996).
- [6] Y.-H. Kim, R. Yu, S. P. Kulik, Y. Shih, and M. O. Scully, *Physical Review Letters* **84**, 1 (2000).
- [7] V. Jacques, E. Wu, F. Grosshans, F. Treussart, P. Grangier, A. Aspect, and J.-F. Roch, *Science* **315**, 966 (2007).
- [8] V. Jacques, E. Wu, F. Grosshans, F. Treussart, P. Grangier, A. Aspect, and J.-F. Roch, *Physical Review Letters* **100**, 220402 (2008).
- [9] X.-s. Ma, J. Kofler, and A. Zeilinger, *Reviews of Modern Physics* **88**, 015005 (2016).
- [10] J.-S. Tang, Y.-L. Li, X.-Y. Xu, G.-Y. Xiang, C.-F. Li, and G.-C. Guo, *Nature Photonics* **6**, 600 (2012).
- [11] F. Kaiser, T. Coudreau, P. Milman, D. B. Ostrowsky, and S. Tanzilli, *Science* **338**, 637 (2012).
- [12] A. Peruzzo, P. Shadbolt, N. Brunner, S. Popescu, and J. L. O’Brien, *Science* **338**, 634 (2012).
- [13] R. Ionicioiu and D. R. Terno, *Physical Review Letters* **107**, 230406 (2011).
- [14] M. O. Scully and K. Drühl, *Physical Review A* **25**, 2208 (1982).
- [15] Y.-H. Kim, R. Yu, S. P. Kulik, Y. Shih, and M. O. Scully, *Physical Review Letters* **84**, 1 (2000).
- [16] T. Jennewein, G. Weihs, J.-W. Pan, and A. Zeilinger, *Physical review letters* **88**, 017903 (2001).
- [17] X.-s. Ma, S. Zotter, J. Kofler, R. Ursin, T. Jennewein, Č. Brukner, and A. Zeilinger, *Nature Physics* **8**, 479 (2012).
- [18] M. O. Scully and M. S. Zubairy, “Quantum optics,” (1999).
- [19] A. Kozhekin, K. Mølmer, and E. Polzik, *Physical Review A* **62**, 033809 (2000).
- [20] J. Nunn, I. Walmsley, M. Raymer, K. Surmacz, F. Waldmann, Z. Wang, and D. Jaksch, *Physical Review A* **75**, 011401 (2007).
- [21] K. Reim, J. Nunn, V. Lorenz, B. Sussman, K. Lee, N. Langford, D. Jaksch, and I. Walmsley, *Nature Photonics* **4**, 218 (2010).
- [22] K. F. Reim, J. Nunn, X.-M. Jin, P. Michelberger, T. Champion, D. G. England, K. Lee, W. Kolthammer, N. Langford, and I. Walmsley, *Physical review letters* **108**, 263602 (2012).
- [23] D.-S. Ding, W. Zhang, Z.-Y. Zhou, S. Shi, B.-S. Shi, and G.-C. Guo, *Nature Photonics* **9**, 332 (2015).
- [24] V. Balić, D. A. Braje, P. Kolchin, G. Yin, and S. E. Harris, *Physical review letters* **94**, 183601 (2005).
- [25] S. Du, J. Wen, and M. H. Rubin, *JOSA B* **25**, C98 (2008).
- [26] M. Fleischhauer and M. D. Lukin, *Physical Review Letters* **84**, 5094 (2000).
- [27] J. Guo, X. Feng, P. Yang, Z. Yu, L. Chen, C.-H. Yuan, and W. Zhang, *Nature Communications* **10**, 148 (2019).